Modulation of quartz-like GeO2 structure by Si substitution: an X-ray diffraction study of Ge1-xSixO2 (0

Adrien Lignie, Dominique Granier, Pascale Armand, Julien Haines, Philippe Papet

Journal of
Applied Crystallography
ISSN 0021-8898
Editor: **Anke R. Kaysser-Pyzalla**

Modulation of quartz-like GeO_2 structure by Si substitution: an X-ray diffraction study of $Ge_{1-x}Si_xO_2$ ($0 \leq x < 0.2$) flux-grown single crystals

Adrien Lignie, Dominique Granier, Pascale Armand, Julien Haines and Philippe Papet

J. Appl. Cryst. (2012). **45**, 272–278

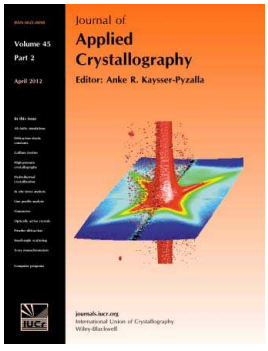

Journal of
Applied Crystallography
ISSN 0021-8898

Received 21 October 2011
Accepted 24 January 2012

Modulation of quartz-like GeO_2 structure by Si substitution: an X-ray diffraction study of $Ge_{1-x}Si_xO_2$ ($0 \leq x < 0.2$) flux-grown single crystals

Adrien Lignie,* Dominique Granier, Pascale Armand, Julien Haines and Philippe Papet

Institut Charles Gerhardt Montpellier, UMR5253 CNRS-UM2-ENSCM-UM1, C2M, UMII, CC1504, Place E. Bataillon, 34095 Montpellier Cedex 5, France. Correspondence e-mail: adrien.lignie@univ-montp2.fr

The spontaneous nucleation by the high-temperature flux method of GeO_2 and SiO_2-substituted GeO_2 ($Ge_{1-x}Si_xO_2$) compounds was improved to give single crystals free of hydroxy groups. The crystal structure and quality of these α-quartz-like piezoelectric materials were studied by single-crystal X-ray diffraction at room temperature. The refinements gave excellent final reliability factors, which are an indication of single crystals with a low level of defects. A good correlation was found between the silicon content in $Ge_{1-x}Si_xO_2$ crystals determined through extrapolation from the inter-tetrahedral bridging angle and that found from energy-dispersive X-ray spectroscopy. The effect of germanium replacement by silicon on the distortion of the α-quartz-type GeO_2 structure was followed by the evolution of the intra-tetrahedral angle and other structural parameters. The TO_4 (T = Si, Ge) distortion was found to be larger in α-GeO_2 than in α-SiO_2 and, as expected, the irregularity of the TO_4 tetrahedra decreased linearly as the substitution of Si for Ge increased.

1. Introduction

In the course of the improvement of piezoelectric performance in terms of the electromechanical coupling coefficient (k^2) and thermal stability, the family of low-temperature quartz-like homeotypes (space groups $P3_221$ or $P3_121$) has been studied in great detail over the past 40 years (O'Connell & Carr, 1977; Wallnofer *et al.*, 1994; Armand *et al.*, 2009; Zhang & Yu, 2011). In the α-quartz-like family of TO_2 (T = Si, Ge) and MXO_4 compounds (M = B, Al, Ga, Fe, Mn; X = P, As), the k coefficient is linearly proportional to the structural distortion (Philippot *et al.*, 1994). From this point of view, it has been shown that the most distorted, and thus the most promising, piezoelectric materials are GeO_2 and $GaAsO_4$ (Philippot *et al.*, 1999). Moreover, owing to the high degree of structural distortion in GeO_2, the transition from α-quartz to β-quartz, as encountered in SiO_2 near 846 K (Kihara, 1990), is absent.

The high structural distortion and room-temperature metastability of the α-quartz structure of GeO_2 make its growth as a single crystal quite difficult. Single crystals of chemical composition $Ge_{1-x}Si_xO_2$ ($0 \leq x < 0.14$) with the α-quartz structure were grown by the reflux method at low temperature in a water medium (Balitsky *et al.*, 2001). A thermal study has shown a phase transition from α-quartz to a rutile-like structure, space group $P4_2/mnm$ (Baur & Khan, 1971), near 463 K for the GeO_2 end-member composition, due to the presence of water inclusions acting as catalysts. This phase transition temperature was found to increase slightly as the replacement of Ge atoms by Si increased up to $x = 0.14$.

In order to overcome the presence of water contamination, the high-temperature flux technique was used to grow OH-free GeO_2-based single crystals with a high visual transparency. Pure GeO_2, with a cubic like morphology, and several compositions of the GeO_2-rich part of the GeO_2–SiO_2 binary diagram, with a hexagonal–prismatic shape, were synthesized in the low-temperature α-quartz phase (Lignie *et al.*, 2011). The growth yield of SiO_2-substituted GeO_2 crystals was found to be two to three times higher than that of the metastable GeO_2 phase. The absence of OH contamination, as detectable by IR spectroscopy, and the high thermal stability of the structure up to its melting point make these flux-grown oxide compounds very promising piezoelectric materials.

However, flux-growth methods are often associated with the formation of flux inclusions in the crystal framework or with the incorporation of chemical impurities from the flux solvent. These foreign elements induce microscopic defects which may cause a deterioration of crystal performance at high temperature. In order to characterize the crystalline quality of these flux-grown materials, a crystal structure study of the α-quartz-type phase of pure GeO_2 and SiO_2-substituted GeO_2 single crystals is necessary.

Table 1
Crystallographic data from room-temperature single-crystal X-ray experiments.

T = Si, Ge. $R_{int} = \sum |(F_o^2) - (\overline{F_o^2})| / \sum (F_o^2)$, $R_1 = \sum ||F_o| - |F_c|| / \sum |F_o|$, $wR_2 = [\sum w(F_o^2 - F_c^2)^2 / \sum w(F_o^2)^2]^{1/2}$, GOF (goodness of fit) = $\{\sum [w(F_o^2 - F_c^2)^2] / (n-p)\}^{1/2}$, where n is the number of reflections, p the total number of refined parameters and w the weighting parameter, with $w = 1/[\sigma^2 F_o^2 + (aP)^2 + bP]$ and $P = [2F_c^2 + \mathrm{Max}(F_o^2, 0)]/3$.

Sample designation	GeO_2	$Ge_{1-x}Si_xO_2$-1	$Ge_{1-x}Si_xO_2$-2	$Ge_{1-x}Si_xO_2$-3	$Ge_{1-x}Si_xO_2$-4	SiO_2
M_r	104.59	103.43	102.71	99.94	96.83	60.09
Crystal system	Trigonal	Trigonal	Trigonal	Trigonal	Trigonal	Trigonal
Space group	$P3_121$ (No. 152)	$P3_221$ (No. 154)	$P3_121$ (No. 152)	$P3_221$ (No. 154)	$P3_121$ (No. 152)	$P3_221$ (No. 154)
Z	3	3	3	3	3	3
Lattice parameters (Å)	a = 4.9890 (3)	a = 4.9830 (1)	a = 4.9805 (2)	a = 4.97517 (17)	a = 4.9707 (3)	a = 4.91636 (19)
	c = 5.6527 (3)	c = 5.6339 (2)	c = 5.6270 (3)	c = 5.60565 (19)	c = 5.5873 (3)	c = 5.40840 (20)
c/a	1.1330 (2)	1.13062 (6)	1.1298 (1)	1.12673 (8)	1.1241 (2)	1.10008 (9)
Volume (Å^3)	121.847 (12)	121.149 (6)	120.880 (9)	120.163 (7)	119.555 (12)	113.210 (7)
$T-O-T$ (°)	130.14 (6)	130.49 (12)	130.72 (9)	131.54 (11)	132.49 (9)	143.625 (5)
Calculated density (g cm^{-3})	4.276	4.253	4.233	4.143	4.035	2.644
Absorption coefficient (cm^{-1})	18.330	17.981	17.735	16.741	15.590	0.994
Crystal volume (mm^3)	0.00039	0.00227	0.00113	0.00321	0.07226	0.00505
hkl indices	$-8 \le h \le 8$	$-7 \le h \le 7$	$-7 \le h \le 7$	$-7 \le h \le 7$	$-7 \le h \le 7$	$-7 \le h \le 7$
	$-8 \le k \le 7$	$-7 \le k \le 7$	$-7 \le k \le 7$	$-7 \le k \le 7$	$-7 \le k \le 7$	$-7 \le k \le 7$
	$-9 \le l \le 9$	$-8 \le l \le 8$	$-8 \le l \le 8$	$-8 \le l \le 8$	$-7 \le l \le 8$	$-8 \le l \le 8$
Angular domain	4.72–37.04	4.72–32.37	4.73–32.57	4.73–32.45	4.74–32.38	4.79–34.79
Reflections collected/unique	2014/410†	2144/283	2157/284	2860/274	2176/277	7027/318
R_{int}	0.0196	0.0317	0.0236	0.0360	0.0258	0.0293
$R\sigma$	0.0125	0.0131	0.0115	0.0158	0.0113	0.0077
R_1 [$I > 2\sigma(I)$]	0.0084	0.0147	0.0099	0.0130	0.0100	0.0131
wR_2 [$I > 2\sigma(I)$]	0.0199	0.0380	0.0241	0.0297	0.0236	0.0401
GOF	1.151	1.181	1.199	1.194	1.220	1.253
Extinction coefficient	0.216 (5)	0.407 (18)	0.302 (9)	0.275 (11)	0.031 (3)	12.8 (4)
Flack parameter	−0.069 (19)	−0.07 (4)	−0.04 (3)	−0.07 (4)	−0.01 (3)	−0.02 (17)
Residual peaks (e Å^{-3})	0.26/−0.33	0.54/−0.42	0.34/−0.43	0.30/−0.29	0.33/−0.29	0.21/−0.26
Density r.m.s.	0.071	0.127	0.086	0.094	0.074	0.064
Weighting parameters	a = 0.0085	a = 0.0168	a = 0.0085	a = 0.0095	a = 0.0064	a = 0.0238
	b = 0.0233	b = 0.2243	b = 0.0833	b = 0.1155	b = 0.0732	b = 0.0151

† The record of GeO_2 data was optimized according to its Laue class ($\bar{3}m$), which gave a higher number of unique reflections.

In this paper, the structural results obtained from room-temperature single-crystal X-ray diffraction (XRD) measurements are reported. In addition, the results from flux-grown GeO_2 and GeO_2–SiO_2 are compared with those of hydrothermally grown SiO_2. The effect of germanium replacement (by silicon) on the α-quartz-type structure is assessed by following the evolution of both the angular distortions and the structural parameters. The inter-tetrahedral angle was found to give a good indication of the silicon content present in the structure, as confirmed by energy-dispersive X-ray spectroscopy (EDX). An attempt is made to find a correlation between the structural parameters and the experimental growth results.

2. Experimental

2.1. Synthesis

GeO_2 and SiO_2-substituted GeO_2 single crystals were grown by spontaneous nucleation in a flux using the slow-cooling growth process, as already reported by Lignie *et al.* (2011). The mixed solutes were obtained in the glassy state for SiO_2/GeO_2 molar ratios of 0.031, 0.053, 0.111 and 0.250. The solute (pure GeO_2 or mixed GeO_2–SiO_2) was dissolved at high temperature in $K_2Mo_4O_{13}$ flux. The supersaturation technique employed was slow cooling between 1243 and 873 K at 1 K h^{-1}. After the dissolution of the flux in a slightly acidic solution, highly transparent colourless and well faceted small single crystals ($\le$3 mm) were present.

A synthetic SiO_2 single crystal grown by the hydrothermal method (Laudise & Nielsen, 1961) was also measured under the same conditions.

2.2. Characterization

Single-crystal XRD experiments were performed on an Xcalibur four-circle diffractometer (Oxford Diffraction) using monochromatic Mo $K\alpha$ radiation (λ = 0.71073 Å) and a CCD detector. Intensity measurements were carried out at room temperature by performing ω scans of Bragg peaks in the range $4.72 \le 2\theta \le 37.04°$.

Structure refinements[1] were carried out using the *SHELXL* program (Sheldrick, 2008), with atomic form factors of neutral atoms from *International Tables for Crystallography* (Wilson, 1992). Only the reliability factors calculated for intense reflections ($|F| > 2\sigma|F|$) are given. The numerical absorption corrections (Gaussian grid integration) were carried out using the *CrysAlis Pro* software (Oxford Diffraction, 2007). The

[1] Supplementary data for this paper are available from the IUCr electronic archives (Reference: CE5127). Services for accessing these data are described at the back of the journal.

resulting atomic positions were standardized using the *StructureTidy* program (Gelato & Parthé, 1987).

The chemical compositions of the XRD-analysed as-grown single crystals were calculated from an average of multiple analyses performed by EDX spectroscopy. At least three different areas were checked for each sample. A Quanta 200 field emission gun (FEI) equipped with an SDD diode was used as detector (Oxford INCA). Spectra were measured under a low vacuum (around 10^{-5} Torr; 1 Torr = 133.322 Pa) at 15 kV.

3. Results and discussion

Flux-grown GeO_2 and mixed $Ge_{1-x}Si_xO_2$ single crystals, as well as a hydrothermally grown SiO_2 crystal, were studied by XRD under ambient conditions. The symmetries and space groups obtained (Table 1) confirm the crystallization of the α-quartz-type structure for all the compositions studied. They belong to the $P3_221$ or $P3_121$ space group, depending on the orientation of the helical axis (right and left, respectively). In the hexagonal unit cell, each cation (Ge^{4+} or Si^{4+}) is surrounded by four oxygen anions in a tetrahedral coordination and each anion is shared between two cations, forming a three-dimensional framework.

The presence of chiral twinning (also called Brazil or optical twins), which is one of the main causes of the deterioration in piezoelectric properties of this low-quartz family (Grassl *et al.*, 2000), was checked. Concerning the studied compositions, the values of the Flack parameters (Flack, 1983; Table 1), which are an indicator of the presence of growth portions containing a mirror image, were close to zero. Furthermore, the *SHELXL* refinements gave excellent final reliability factors (Table 1), indicating that the single crystals are of high quality and thus precluding the presence of any significant degree of twinning.

Optical twinning was also investigated on the as-grown GeO_2 (Fig. 1) and mixed (Fig. 2) single crystals using polarized light. The uniform coloration of the natural faces under polarized light [Figs. 1(*b*) and 1(*c*), and Figs. 2(*b*) and 2(*c*)] indicates the lack of optical domains in the flux-grown GeO_2-based materials.

Since the samples used for these single-crystal X-ray characterizations (around 0.014 mm^3) were not large enough for reliable chemical composition analysis, we used the $T-O-T$ (T = Si, Ge) inter-tetrahedral bridging angle θ (Table 1) to quantify the Si content x of the mixed flux-grown $Ge_{1-x}Si_xO_2$ single crystals. These angles were found to be linearly dependent on substitution in $AlPO_4$–$GaPO_4$ solid solutions (Haines *et al.*, 2004) and for some compositions of GeO_2–SiO_2 solid solutions in the silicon-rich part (Ranieri *et al.*, 2011). The $T-O-T$ angle represents the angle between two corner-sharing TO_4 tetrahedral units. In addition, this θ angle is geometrically linked to the tilt angle δ, which corresponds to

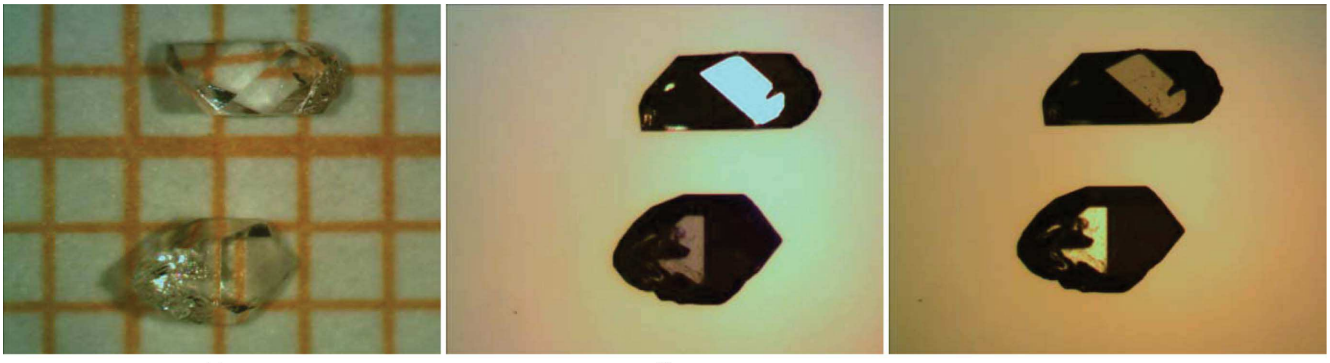

(*a*) (*b*) (*c*)

Figure 1
Photographs of as-grown GeO_2 crystals: (*a*) without and (*b*) and (*c*) with polarized light.

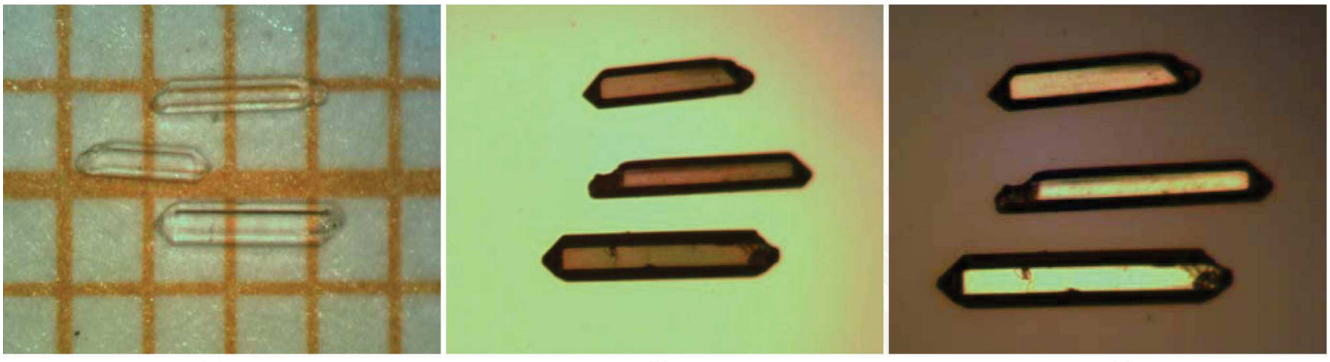

(*a*) (*b*) (*c*)

Figure 2
Photographs of as-grown mixed crystals: (*a*) without and (*b*) and (*c*) with polarized light.

Table 2
Results of the EDX analyses in atomic percent and comparison of the silicon atomic composition x of $Ge_{1-x}Si_xO_2$ obtained from EDX and θ interpolation.

	$Ge_{1-x}Si_xO_2$-1	$Ge_{1-x}Si_xO_2$-2	$Ge_{1-x}Si_xO_2$-3	$Ge_{1-x}Si_xO_2$-4
At.% from EDX analyses	Ge: 32.33 (21) Si: 0.69 (3) O: 66.98 (21)	Ge: 35.82 (24) Si: 1.30 (12) O: 62.88 (27)	Ge: 27.40 (17) Si: 3.07 (10) O: 69.53 (21)	Ge: 25.56 (75) Si: 5.72 (10) O: 68.72 (75)
x from EDX	2.1 (1)%	3.5 (3)%	10.1 (4)%	18.3 (7)%
x extrapolated from θ	2.6 (21)%	4.3 (18)%	10.4 (19)%	17.4 (17)%

the tilting of the TO_4 tetrahedra about the x axis compared with an idealized β-quartz structure (Philippot *et al.*, 1999; Grimm & Dorner, 1975).

A linear relationship between the inter-tetrahedral bridging angle data for pure GeO_2 and SiO_2 was assumed (Fig. 3). The $T-O-T$ angles obtained from a first set of refinements performed with the Si-content parameter allowed to refine freely were used to interpolate the Si content x of the mixed $Ge_{1-x}Si_xO_2$ single crystals, as plotted in Fig. 3. Compared with the standard errors on the inter-tetrahedral bridging angles (Table 1), the errors on the silicon composition x from the interpolation of θ are quite large (Table 2).

Next, a second set of refinements was performed with the Si content fixed to this estimated value. Whatever the mixed sample composition, the final value of θ was very similar to that of the first refinement, *i.e.* the final inter-tetrahedral angle lay within the error range of the first one. The results of the second and final refinements are presented in Tables 1 and 3–5.

The same method has already been applied for mixed $Ge_{1-x}Si_xO_2$ single crystals grown in the SiO_2-rich part of the GeO_2–SiO_2 solid solution, *i.e.* for Si contents x in the range 0.87–0.93 (Ranieri *et al.*, 2011). Their $T-O-T$ angle values are also reported in Fig. 3.

In order to validate this method of Si-content determination based on the inter-tetrahedral angle, the chemical composition of the flux-grown mixed crystals was analysed using EDX. These EDX measurements (Table 2) were performed on a new set of large samples from the same synthesis batch as the samples analysed by XRD. From these EDX atomic percent data, the Si atomic composition x in the mixed $Ge_{1-x}Si_xO_2$ single crystals was calculated (Table 2) and compared with the chemical composition obtained by interpolation from the initial θ values. Taking into account the errors on the results, there is very good agreement between the chemical compositions x obtained from the EDX measurements and from the interpolation of θ.

The values of the unit-cell volume V and lattice parameters a and c are in very good agreement with those found in the literature for the two end members of the GeO_2–SiO_2 solid solution (Haines *et al.*, 2002; Glinneman *et al.*, 1992). Compared with pure GeO_2, the reduction in the V, a and c parameters with increasing silicon content in the $Ge_{1-x}Si_xO_2$-z crystals (entries with z = 1–4 in Table 1) indicates an efficient substitution of silicon for germanium. Very low values of the agreement factors R were also found for $Ge_{1-x}Si_xO_2$ compounds (Table 1), even for the highest SiO_2-substituted GeO_2 compositions (entries $Ge_{1-x}Si_xO_2$-3 and $Ge_{1-x}Si_xO_2$-4; Table 2).

Replacement of germanium by silicon induces a compression of the unit cell corresponding to a reduction in volume V (Table 1). In order to highlight this phenomenon, the decreases in the a and c lattice parameters are plotted *versus* Si content x in Fig. 4. The three reported data points corresponding to hydrothermally grown $Ge_{1-x}Si_xO_2$ compositions with a very high Si content (asterisks) are taken from Ranieri

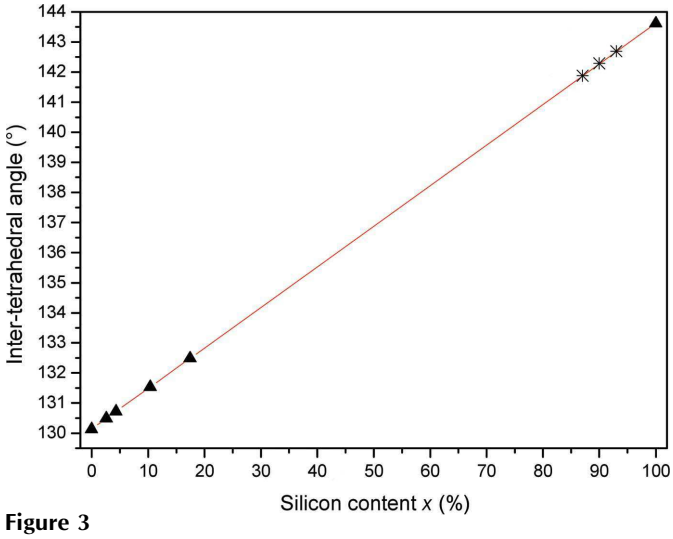

Figure 3
Determination of the Si content x in flux-grown $Ge_{1-x}Si_xO_2$ single crystals by interpolation of the inter-tetrahedral angles between GeO_2 and SiO_2 (triangles). The three hydrothermally grown $Ge_{1-x}Si_xO_2$ compositions with a very high Si content (asterisks) are data taken from Ranieri *et al.* (2011). The error bars are smaller than the symbol size.

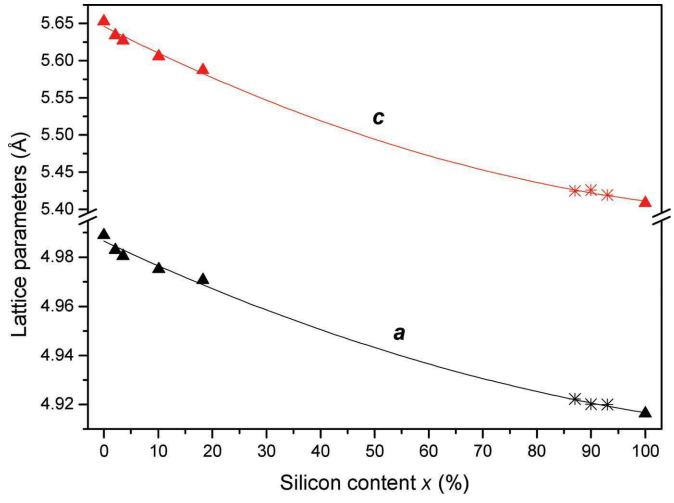

Figure 4
Evolution of unit-cell parameters a and c with silicon content x. Solid lines are second-order least-squares fits to the data. The three hydrothermally grown $Ge_{1-x}Si_xO_2$ compositions with a very high Si content (asterisks) are data taken from Ranieri *et al.* (2011). The error bars are smaller than the symbol size.

Table 3
T—O bond lengths (Å) and O—T—O intra-tetrahedral angles (°) (T = Si, Ge) and their related distortion indices (DIs).

Distortion indices are defined as $(\sum_{i=1}^{n} |y_i - \langle y \rangle|)/(n\langle y \rangle)$, with y_i the individual and $\langle y \rangle$ the mean tetrahedral bond lengths or intra-tetrahedral angles (Baur, 1974). The silicon atomic composition is given by x. Standard deviations are in parentheses.

	GeO_2	x = 0.026	x = 0.043	x = 0.104	x = 0.174	SiO_2
d_{T-O} (×2)	1.7350 (10)	1.7290 (20)	1.7268 (15)	1.7180 (20)	1.7053 (15)	1.6075 (8)
(×2)	1.7436 (8)	1.7372 (18)	1.7333 (12)	1.7226 (15)	1.7158 (12)	1.6128 (7)
$\langle d_{T-O} \rangle$	1.7394	1.7331	1.7300	1.7203	1.7106	1.6102
DI (T—O)	0.0025	0.0024	0.0019	0.0013	0.0031	0.0016
O—T—O (×1)	107.79 (6)	107.72 (13)	107.83 (9)	108.12 (12)	108.08 (9)	108.95 (6)
(×2)	106.33 (2)	106.48 (5)	106.50 (3)	106.63 (4)	106.91 (3)	108.75 (2)
(×2)	112.96 (5)	112.96 (11)	112.87 (8)	112.60 (10)	112.57 (7)	110.53 (4)
(×1)	110.56 (6)	110.33 (13)	110.36 (9)	110.34 (12)	109.87 (9)	109.34 (5)
$\langle$O—T—O$\rangle$	109.488	109.488	109.488	109.487	109.485	109.475
DI (O—T—O)	0.0244	0.0237	0.0232	0.0216	0.0200	0.0060

Table 4
Fractional atomic coordinates (space group $P3_121$, or space group $P3_221$ for compositions marked with an asterisk) and equivalent isotropic displacement parameters U_{eq} (Å^2).

The silicon composition of the solid solutions is given by the x parameter. Standard uncertainties are given in parentheses.

	GeO_2	x = 0.026*	x = 0.043	x = 0.104*	x = 0.174	SiO_2*
$x_{Ge/Si}$	0.45123 (3)	0.45171 (8)	0.45197 (5)	0.45280 (7)	0.45366 (6)	0.46973 (7)
$100U_{eq}$(Ge/Si)	0.678 (5)	0.759 (16)	0.749 (10)	0.885 (13)	0.800 (8)	0.691 (16)
x_O	0.60270 (20)	0.6025 (5)	0.6020 (3)	0.6003 (4)	0.5998 (3)	0.58646 (17)
y_O	0.90480 (20)	0.9033 (5)	0.9025 (4)	0.8995 (4)	0.8957 (3)	0.85404 (17)
z_O	0.09049 (14)	0.9033 (3)	0.0917 (2)	0.9068 (3)	0.09513 (2)	0.88090 (12)
$100U_{eq}$(O)	1.200 (16)	1.26 (3)	1.29 (2)	1.45 (3)	1.45 (2)	1.245 (18)

et al. (2011). The behaviour was fitted to a second-degree polynomial over the whole GeO_2–SiO_2 solid solution range:

$$a\ (\text{Å}) = 4.9866 - 1.04 \times 10^{-4}(x) + 3.37 \times 10^{-6}(x)^2 \quad (1)$$

and

$$c\ (\text{Å}) = 5.6460 - 3.72 \times 10^{-3}(x) + 1.37 \times 10^{-5}(x)^2. \quad (2)$$

From the coefficients of these relationships, it is clear that a preferential contraction occurs along c with Si substitution in α-quartz GeO_2. This preferential distortion is similar to that already observed with increasing temperature for GeO_2 powder and flux-grown SiO_2-substituted GeO_2 single crystals (Haines *et al.*, 2002; Armand *et al.*, 2011).

A second-order polynomial was necessary to fit the lattice parameters (Fig. 4). This deviation from Vegard's (1921) law may be explained by the fact that the α-quartz phase of GeO_2 is not a thermodynamically stable phase under ambient conditions. Furthermore, the significant curvature of both the a and c slopes in the low-SiO_2 content range ($0 \leq x < 0.05$) may also be attributed to GeO_2 metastability. Indeed, the reduction in the nonlinear behaviour of the lattice parameters as Ge atoms are replaced by Si atoms ($0 \leq x < 0.18$) would reflect an improvement in the stability of the α-quartz-like structure which could be directly related to the experimental growth results (Lignie *et al.*, 2011). Compared with pure GeO_2, the spontaneous nucleation of SiO_2-substituted GeO_2 compounds was found to be easier, *i.e.* larger single crystals were obtained in higher yields. The influence of the substitution was also clearly seen on the crystal morphology: hexagonal-like prisms of $Ge_{1-x}Si_xO_2$ were grown, as shown in Fig. 2, whereas tiny GeO_2 crystals were obtained in a pseudo-cubic form, as shown in Fig. 1.

It has been shown that, in the α-quartz structure, the TO_4 (T = Si, Ge) tetrahedra can be strictly regular only if the axial ratio c/a is 1.0981 (Smith & Alexander, 1963). The c/a ratio is 1.1001 for SiO_2, in agreement with Smith & Alexander (1963), and 1.1330 for GeO_2, as already found by Smith & Isaacs (1964). It appears that the TO_4 tetrahedra are more distorted in GeO_2 than in SiO_2 and, as expected, the irregularity of the TO_4 tetrahedra decreases linearly as the substitution of Si for Ge increases, and the c/a ratio decreases.

Linear extrapolation between the c/a value obtained for flux-grown GeO_2 and that for hydrothermally grown SiO_2 (Table 1) gives the following relation:

$$c/a = 1.1330 - 3.292 \times 10^{-4}(x). \quad (3)$$

On the other hand, linear regression in the $0 \leq x < 0.174$ Si-content domain of the c/a ratio of the flux-grown $Ge_{1-x}Si_xO_2$ crystal gives

$$c/a = 1.1330 - 5.03 \times 10^{-4}(x). \quad (4)$$

Comparing equations (3) and (4), we observed that a partial replacement of Ge atoms in α-quartz GeO_2 greatly stabilizes the TO_4 (T = Si, Ge) tetrahedra. Indeed, the c/a values for flux-grown $Ge_{1-x}Si_xO_2$ crystals decrease faster than a simple extrapolation between the two end members of the GeO_2–SiO_2 solid solution. The c/a variation for the SiO_2-substituted GeO_2 materials studied here does not follow Vegard's law. The slope value of the linear regression between pure GeO_2 and the mixed-4 composition ($Ge_{0.826}Si_{0.174}O_2$) is 50% higher than the slope of the linear extrapolation.

Table 3 summarizes the interatomic distances and the intra-tetrahedral angles in the two binary references and in the mixed single crystals. The value of the average T—O (T = Si, Ge) bond length tends to decrease linearly from GeO_2 to SiO_2. To quantify the deviations from a regular TO_4 tetrahedron (T = Si, Ge), distortion indices can be calculated, defined as the sum of the average deviations from their mean values (Baur, 1974) (Table 3). The distortion of the GeO_4 tetrahedra in α-GeO_2, as reported by Smith & Isaacs (1964), is a result of unequal O—Ge—O bond angles rather than unequal Ge—O distances. This is clearly expressed by the distortion indices of the intra-tetrahedral angles, which are one order of magnitude

Table 5
U_{ij} values (Å^2) of the anisotropic displacement parameters as a function of silicon content x.

		GeO_2	x = 0.026	x = 0.043	x = 0.104	x = 0.174	SiO_2
$U_{11} \times 100$	Ge/Si	0.757 (7)	0.833 (18)	0.832 (12)	0.968 (16)	0.867 (11)	0.752 (18)
	O	1.71 (4)	1.75 (9)	1.72 (7)	1.83 (9)	1.80 (6)	1.62 (3)
$U_{22} \times 100$	Ge/Si	0.637 (8)	0.73 (2)	0.730 (14)	0.879 (19)	0.796 (14)	0.582 (19)
	O	1.21 (4)	0.92 (8)	1.09 (6)	1.47 (8)	1.47 (6)	1.18 (3)
$U_{33} \times 100$	Ge/Si	0.601 (6)	0.680 (19)	0.652 (12)	0.778 (16)	0.714 (11)	0.68 (2)
	O	1.05 (3)	1.27 (7)	1.15 (5)	1.28 (6)	1.33 (5)	1.25 (3)
$U_{23} \times 100$	Ge/Si	0.040 (6)	−0.038 (12)	0.042 (10)	0.056 (13)	−0.057 (10)	−0.015 (9)
	O	0.45 (3)	−0.04 (7)	−0.07 (5)	0.51 (6)	−0.47 (4)	−0.44 (2)
$U_{13} \times 100$	Ge/Si	0.020 (3)	−0.019 (6)	0.021 (5)	0.028 (7)	−0.029 (5)	−0.008 (4)
	O	0.43 (3)	−0.50 (7)	0.39 (5)	0.37 (6)	−0.30 (5)	−0.29 (2)
$U_{12} \times 100$	Ge/Si	0.319 (4)	0.365 (10)	0.365 (7)	0.439 (10)	0.398 (7)	0.291 (10)
	O	1.01 (4)	0.76 (7)	0.78 (5)	1.02 (8)	1.01 (6)	0.94 (3)

larger than the distortion indices of the first-shell distances, whatever the chemical composition studied (Table 3).

Only a slight evolution of the distortion indices of the T—O distances is observed when going from GeO_2 to SiO_2 compositions, *i.e.* as the Si content increases in the quartz structure (Table 3), while a stronger decrease in the distortion indices of the intra-tetrahedral angles can be noted. This evolution is representative of the tendency of the O—T—O intra-tetrahedral angles to approach the ideal value of 109.5°, characteristic of a perfectly regular tetrahedron (Smith & Alexander, 1963; see Fig. 5). In other words, the reduction in the distortion, also indicated by the decrease in the c/a ratio, for the mixed flux-grown compounds is essentially due to the reduction of the O—T—O angles and the increase of the T—O—T angle. Taking into account the reported data concerning the Si-rich part (Ranieri *et al.*, 2011), the linear variation of the intra-tetrahedral angles appears to cover the whole range of the GeO_2–SiO_2 solid solution (Fig. 5).

Normalized fractional atomic coordinates, according to Wyckoff positions, and isotropic displacement parameters are given in Table 4. The Ge and Si atoms lie on the 3*a* special position ($x_{Ge/Si}$, 0, $\frac{1}{3}$) for space group $P3_121$ and ($x_{Ge/Si}$, 0, $\frac{2}{3}$) for space group $P3_221$. The O atoms occupy the 6*c* general position (x_O, y_O, z_O). There are three formula units per unit cell. The atomic coordinates of the Ge and Si atoms at ambient pressure and temperature agree very well with those already published for GeO_2 and SiO_2 single crystals by Kihara (1990) and Glinneman *et al.* (1992).

The x coordinate of the Ge/Si atoms increases as the x_O, y_O and z_O O-atom coordinates decrease when going from GeO_2 to SiO_2. This is consistent with the decreased tilt of the TO_4 tetrahedra when Si replaces Ge in the solid solutions.

The U_{ij} values of the anisotropic displacement parameters of the refined structures of the single-crystal samples are presented in Table 5. The magnitudes found for the pure GeO_2 and SiO_2 quartz compositions are in good agreement with those given by previous authors (Glinneman *et al.*, 1992). The comparison of U_{ij} values (Table 5) and U_{eq} values (Table 4) show some deviations, indicating that the Ge/Si movements above their equilibrium positions are essentially isotropic, in contrast with O (Haines *et al.*, 2002; Glinneman *et al.*, 1992; Smith & Isaacs, 1964).

An increase in the U_{ij} values is observed for the $Ge_{1-x}Si_xO_2$ compounds compared with those of the end members of the GeO_2–SiO_2 solid solution. This could be directly attributed to the presence of a slight structural disorder caused by the substitution of Si atoms for Ge atoms in the α-quartz-like GeO_2 structure.

For all the studied compositions, the values of U_{11} are larger than those of U_{22} and U_{33}. This has been shown previously for quartz (Kihara, 1990) and attributed to librational motion of O in Si—O—Si linkages around the Si—Si axis (Kihara, 1993).

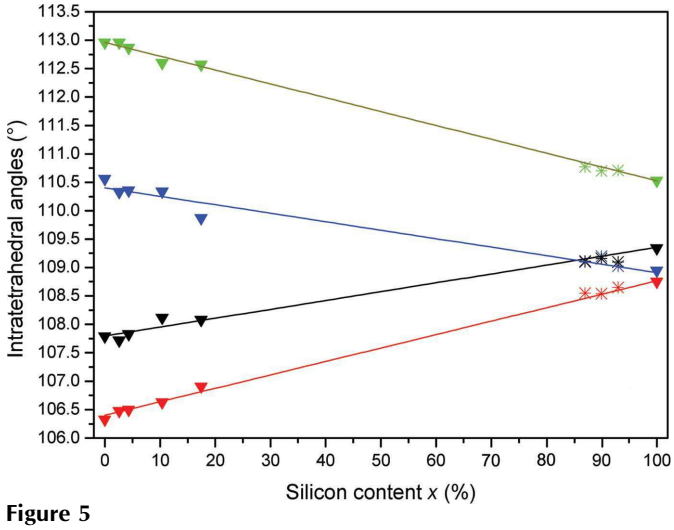

Figure 5
Evolution of the intra-tetrahedral angles with Si content x for $Ge_{1-x}Si_xO_2$ crystals. Triangles denote data from the present work, and asterisks are data taken from Ranieri *et al.* (2011). The error bars are smaller than the symbol size.

4. Conclusions

In order to characterize the crystalline quality of high-temperature flux-grown GeO_2-based materials, a crystal structure study was undertaken based on room-temperature single-crystal X-ray diffraction measurements (XRD). The refinement results confirm crystallization in the trigonal system for pure GeO_2 and mixed $Ge_{1-x}Si_xO_2$ single crystals. The very low values of the agreement factors, as well as the absence of optical twins, are consistent with flux-grown single crystals presenting a low level of defects.

The linear variation of the inter-tetrahedral angle was used to estimate the degree of substitution in the solid solutions. This method was found to be effective based on a comparison with the EDX results.

The effect of Ge replacement by Si on the distortion of the α-quartz-type GeO_2 structure was assessed by following the evolution of the intra-tetrahedral angles and other structural parameters. With an increase in the substitution rate, the irregularity of the intra-tetrahedral angles of GeO_2 decreases faster than expected. As this structural distortion is also

directly related to the piezoelectric properties of the α-quartz family (Philippot *et al.*, 1994), its decrease should mean a decrease in the piezoelectric performance of the solid solutions.

This XRD study has shown the high purity and high crystalline quality of millimetre-sized GeO_2-based crystals obtained from the flux method. However, centimetre-sized single crystals need to be obtained in order to measure their piezoelectric properties and thus to confirm the promising potential of α-quartz GeO_2. If the correlation between intertetrahedral angles and electromechanical coupling coefficients is confirmed, the silicon content in $Ge_{1-x}Si_xO_2$ single crystals should be optimized in order to find the best compromise between size/yield and electromechanical coupling coefficient.

References

Armand, P., Beaurain, M., Rufflé, B., Menaert, B. & Papet, P. (2009). *Inorg. Chem.* **48**, 4988–4996.

Armand, P., Clément, S., Balitsky, D., Lignie, A. & Papet, P. (2011). *J. Cryst. Growth*, **316**, 153–157.

Balitsky, D. V., Balitsky, V. S., Pisarevsky, Y. V., Philippot, E., Silvestrova, O. Y. & Pushcharovsky, D. Y. (2001). *Ann. Chim. Sci. Mater.* **26**, 183–192.

Baur, W. H. (1974). *Acta Cryst.* B**30**, 1195–1215.

Baur, W. H. & Khan, A. A. (1971). *Acta Cryst.* B**27**, 2133–2139.

Flack, H. D. (1983). *Acta Cryst.* A**39**, 876–881.

Gelato, L. M. & Parthé, E. (1987). *J. Appl. Cryst.* **20**, 139–143.

Glinneman, J., King, H. E., Schultz, H., Hahn, Th., La Placa, S. J. & Dacol, F. (1992). *Z. Kristallogr.* **198**, 177–212.

Grassl, M., Barz, R. U. & Gille, P. (2000). *J. Cryst. Growth*, **220**, 522–530.

Grimm, H. & Dorner, B. (1975). *Phys. Chem. Solids*, **36**, 407–413.

Haines, J., Cambon, O., Cachau-Herreillat, D., Fraysse, G. & Mallasagne, F. E. (2004). *Solid State Sci.* **6**, 995–999.

Haines, J., Cambon, O., Philippot, E., Chapon, L. & Hull, S. (2002). *J. Solid State Chem.* **166**, 434–441.

Kihara, K. (1990). *Eur. J. Mineral.* **2**, 63–77.

Kihara, K. (1993). *Phys. Chem. Miner.* **19**, 492–501.

Laudise, R. A. & Nielsen, J. W. (1961). *Solid State Phys.* **12**, 149–222.

Lignie, A., Armand, P. & Papet, P. (2011). *Inorg. Chem.* **50**, 9311–9317.

O'Connell, R. M. & Carr, P. (1977). *IEEE Trans. Sonics Ultrason.* **24**, 376–384.

Oxford Diffraction (2007). *CrysAlis Pro*. Version 1.171.32. Oxford Diffraction Ltd, Abingdon, England.

Philippot, E., Armand, P., Yot, P., Cambon, O., Goiffon, A., McIntyre, G. J. & Bordet, P. (1999). *J. Solid State Chem.* **146**, 114–123.

Philippot, E., Goiffon, A., Ibanez, A. & Pintard, M. (1994). *J. Solid State Chem.* **110**, 356–362.

Ranieri, V., Darracq, S., Cambon, M., Haines, J., Cambon, O., Largeteau, A. & Demazeau, G. (2011). *Inorg. Chem.* **50**, 4632–4639.

Sheldrick, G. M. (2008). *Acta Cryst.* A**64**, 112–122.

Smith, G. S. & Alexander, L. E. (1963). *Acta Cryst.* **16**, 462–471.

Smith, G. S. & Isaacs, P. B. (1964). *Acta Cryst.* **17**, 842–846.

Vegard, L. (1921). *Z. Phys. A*, **5**, 17–26.

Wallnofer, W., Krempl, P. W. & Asenbaum, A. (1994). *Phys. Rev. B*, **49**, 10075–10080.

Wilson, A. J. C. (1992). Editor. *International Tables for Crystallography*, Vol. C, pp. 263–271. Dordrecht: Kluwer Academic Publishers.

Zhang, S. & Yu, F. (2011). *J. Am. Ceram. Soc.* **94**, 3153–3170.